

# Whole-lithosphere shear during oblique rifting

Brandon M. Lutz<sup>1</sup>, Gary J. Axen<sup>1</sup>, Jolante W. van Wijk<sup>1,2</sup> and Fred M. Phillips<sup>1</sup><sup>1</sup>Earth and Environmental Science Department, New Mexico Institute of Mining and Technology, 801 Leroy Place, Socorro, New Mexico 87801, USA<sup>2</sup>Los Alamos National Laboratory, Los Alamos, New Mexico 87544, USA

## ABSTRACT

Processes controlling the formation of continental whole-lithosphere shear zones are debated, but their existence requires that the lithosphere is mechanically coupled from base to top. We document the formation of a dextral, whole-lithosphere shear zone in the Death Valley region (DVR), southwest United States. Dextral deflections of depth gradients in the lithosphere-asthenosphere boundary and Moho are stacked vertically, defining a 20–50-km-wide, lower lithospheric shear zone with ~60 km of shear. These deflections underlie an upper-crustal fault zone that accrued ~60 km of dextral slip since ca. 8–7 Ma, when we infer that whole-lithosphere shear began. This dextral offset is less than net dextral offset on the upper-crustal fault zone (~90 km, ca. 13–0 Ma) and total upper-crustal extension (~250 km, ca. 16–0 Ma). We show that, before ca. 8–7 Ma, weak middle crust decoupled upper-crustal deformation from deformation in the lower crust and mantle lithosphere. Between 16 and 7 Ma, detachment slip thinned, uplifted, cooled, and thus strengthened the middle crust, which is exposed in metamorphic core complexes collocated with the whole-lithosphere shear zone. Midcrustal strengthening coupled the layered lithosphere vertically and therefore enabled whole-lithosphere dextral shear. Where thick crust exists (as in pre-16 Ma DVR), midcrustal strengthening is probably a necessary condition for whole-lithosphere shear.

## INTRODUCTION

Continental rupture requires shear zones that cut the entire lithosphere. However, where crust is overthickened, the upper crust is commonly decoupled from lower crust and mantle lithosphere (LCML) by a weak middle crust (Burchfiel and Royden, 1985; Block and Royden, 1990), precluding localized whole-lithosphere shear.

We describe the development of a whole-lithosphere shear zone that formed during dextral-oblique continental extension that overprinted a thrust belt in the Death Valley region (DVR) of the central Basin and Range, United States (Fig. 1). This shear zone forms the northeastern edge of the southern Walker Lane belt (inset in Fig. 1A) and is defined by offset features that span the upper crust to the LCML. Vertically stacked, subparallel, dextral-sense deflections of depth gradients in the Moho ( $62 \pm 17$  km) and lithosphere-asthenosphere boundary (LAB;  $56 \pm 6$  km; Figs. 1B and 1C; Figs. S4–S8 and Table S5 in the Supplemental Material<sup>1</sup>) underlie

two upper-crustal faults with  $57 \pm 7$  km of post-8–7 Ma dextral slip (Figs. 1A and 1C; Fig. S9).

Crust-mantle coupling and development of localized, whole-lithosphere shear zones have been associated with high strain rates, high degrees of rift obliquity, and weak intraplate rheology (Sobolev et al., 2005; Umhoefer, 2011; Brune et al., 2012; Bennett and Oskin, 2014), factors that are rarely well constrained. Using a high-resolution tectonic reconstruction (Lutz, 2021) combined with existing thermochronometry (Fig. S3; Table S4) and thermokinematic modeling (Lutz et al., 2021), we assessed the relative influence of the three factors on whole-lithosphere shear.

We show that thinning, cooling, partial to total exhumation, and strengthening of weak middle crust (i.e., changing rheology), achieved by detachment faulting, were necessary for whole-lithosphere shear in the DVR. These processes, collectively termed “midcrustal strengthening,” coupled the upper crust to the LCML and enabled whole-lithosphere shear.

Midcrustal strengthening incorporates processes previously described as “occlusion” (Wernicke, 1992), “freezing” (Block and Royden, 1990), and “annealing” (Pérez-Gussinyé and Reston, 2001), which have been inferred conceptually (Wernicke, 1992) and modeled analytically (Buck, 1991) and numerically (Rosenbaum et al., 2005). The thermo-kinematic evolution of the DVR and its relationship to offset LAB/Moho depth gradients (Figs. 1B and 1C; Figs. S4–S8) indicate that midcrustal strengthening is required for integrated continental rupture in previously thickened crust.

## UPPER-CRUSTAL MIOCENE–HOLOCENE KINEMATICS OF THE CENTRAL BASIN AND RANGE

Neogene upper-crustal extension in the central Basin and Range was reconstructed by realigning fault-bounded mountain ranges that contain offset features (e.g., Wernicke et al., 1988; McQuarrie and Wernicke, 2005; Lutz, 2021). We followed the method of Lutz (2021), using a reconstruction generated in GPlates (<https://www.gplates.org>; Müller et al., 2018). Euler pole rotations described the relative range-block motions (Tables S1–S3), which were based upon a comprehensive database of offset features, geodetic slip rates, and synextensional basins (see Video S2). Block separations interpolated in 0.1 m.y. time steps yielded extensional velocities. Velocity magnitude and azimuth were related to strain rate (see Video S3) and obliquity (Fig. 2B), respectively, which we compared to the initiation of whole-lithosphere shear at ca. 8–7 Ma (Figs. 1–3).

Previous reconstructions (citations above) show that average Sierra Nevada–Colorado Plateau relative velocity slowed with time (Fig. 2A) and rotated clockwise (Fig. 2B) before and during onset of whole-lithosphere shear. From

<sup>1</sup>Supplemental Material. Description of kinematic reconstruction, reconstructions of the LAB and Moho depth gradients, and three supporting videos of the high-resolution kinematic reconstruction of Lutz (2021). Please visit <https://doi.org/10.1130/G49603.1> to access the supplemental material, and contact [editing@geosociety.org](mailto:editing@geosociety.org) with any questions.

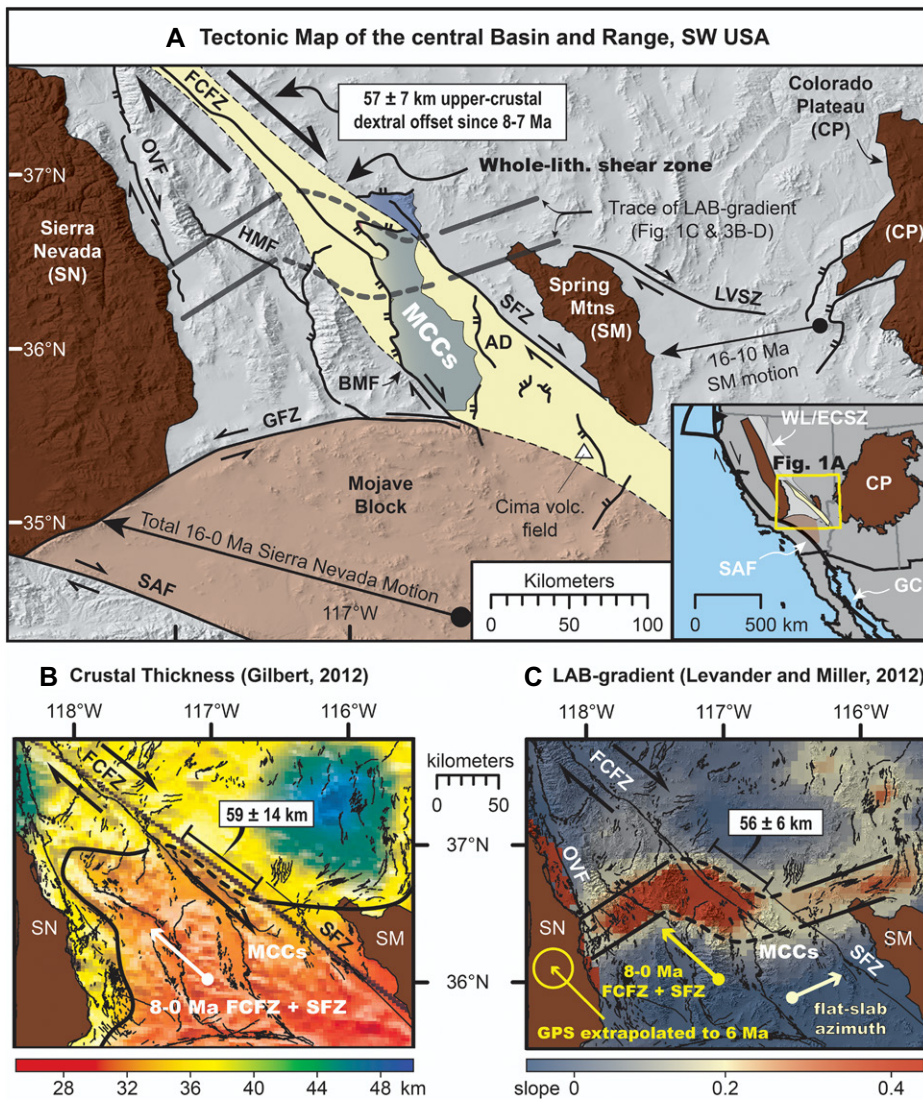


**Figure 1.** Maps of (A) the central Basin and Range and (B–C) the Death Valley region (DVR) of the United States showing whole-lithosphere shear zone (light yellow) collocated with the metamorphic core complex (MCC) belt (blue). Sierra Nevada (SN) and Spring Mountains (SM) are shown in all three maps. Kinematic modeling (Lutz, 2021) of offset features (black in Video S1; Figs. S3 and S9 [see footnote 1]) along Furnace Creek (FCFZ) and Stateline (SFZ) fault zones indicates  $57 \pm 7$  km of post-8–7 Ma slip, equal to deflections in the Moho (B) and lithosphere-asthenosphere boundary (LAB) depth gradient (C). Double half-arrows and tick marks show strike-slip sense and detachment upper plates, respectively. AD—Amargosa detachment breakaway; BMF—Black Mountains fault zone; GPS—global positioning system; HMF—Hunter Mountain fault zone; LVSZ—Las Vegas Valley shear zone; OVF—Owens Valley fault zone; GFZ—Garlock fault zone; SAF—San Andreas fault zone; GC—Gulf of California; WL/ECSZ—Walker Lane/Eastern California shear zone.

Lutz (2021) (see also Fig. 2; Video S3), average extension rate declined from  $\sim 25$  mm/yr ( $\sim 4.5 \times 10^{-15}$  s $^{-1}$ ) at ca. 16 Ma to  $\sim 7.5$  mm/yr ( $\sim 5.5 \times 10^{-16}$  s $^{-1}$ ) at ca. 7 Ma and then increased to  $\sim 11.5$  mm/yr ( $\sim 9.5 \times 10^{-16}$  s $^{-1}$ ) by ca. 2–1 Ma. Obliquity increased at ca. 12 Ma, when Sierra Nevada–Colorado Plateau relative motion rotated from azimuth  $\sim 260^\circ$  to  $\sim 295^\circ$  (Fig. 2B). This clockwise rotation was due to slowing of south-southwest-directed extension east of the Spring Mountains and acceleration of west-northwest-directed extension west of the mountains (Fig. 2C). Subsequently, obliquity

increased as velocity rotated clockwise an additional  $\sim 24^\circ$  from ca. 10 to 7 Ma, mostly from 8 to 7 Ma ( $18^\circ$ ). The ca. 8–7 Ma rotation is based on reconstruction of a  $7.6 \pm 0.3$  Ma (K–Ar) pluton crosscut by the Furnace Creek fault zone (FCFZ; Oakes, 1987). Older (ca. 12–8 Ma) extension was more west-northwest, based on reconstructed Jurassic batholiths, thrust belt features, and synextensional basins (see Videos S1–S3; Fig. S9; Table S1).

Intraplate tectonic changes resolved by the kinematic models (Fig. 2) coincide with changes in Pacific–North American plate-boundary kine-

matics. Post-12 Ma, west-northwest-directed (average azimuth  $\sim 305^\circ$ ; Fig. 2B) extension in the DVR was nearly parallel to reconstructed motions in the northern Gulf of California ( $\sim 310^\circ$ ; Oskin et al., 2001; Bennett and Oskin, 2014). Net Sierra Nevada–Colorado Plateau velocity decreased by  $\sim 8$  mm/yr at ca. 7 Ma (Fig. 2C), within  $\sim 1$  m.y. of the time when dextral plate-boundary motion relocated onto the southern San Andreas fault from a position offshore (ca. 6 Ma; Oskin and Stock, 2003). The decrease likely reflects localization of plate-boundary shear onto the newly reorganized and lengthened San Andreas fault (Wernicke and Snow, 1998). Sierra Nevada–Colorado Plateau and Pacific–North American velocity azimuths converged until they became parallel at ca. 7 Ma (Fig. 2B), about when we infer whole-lithosphere shear initiated. Total Sierra Nevada–Colorado Plateau shear after 7 Ma ( $\sim 58$  km; Lutz, 2021) is similar to net dextral shear in the Mojave block ( $\sim 62$  km; Dixon and Xie, 2018), suggesting that most Mojave dextral shear accrued since ca. 7 Ma.

### WHOLE-LITHOSPHERE DEXTRAL SHEAR SINCE 8–7 MA

Offset features in the upper crust, the Moho, and the LAB define an  $\sim 20$ – $50$ -km-wide, whole-lithosphere shear zone (Fig. 1), in which the entire vertical lithospheric column was sheared dextrally  $\sim 60$  km after ca. 8–7 Ma (Figs. 4B and 4C). Apparent dextral deflections of Moho and LAB depth gradients (Figs. 1B and 1C) underlie and are subparallel to the upper-crustal Furnace Creek and Stateline fault zones. Dextral deflections of Moho and LAB depth gradients suggest  $62 \pm 17$  km (Figs. S5–S8) and  $56 \pm 6$  km (Fig. S4) of dextral shear (toward  $\sim 310^\circ$ – $315^\circ$ ), respectively. Upper-crustal kinematics (Lutz, 2021; Animation 1; Fig. S9) predict that, after 8–7 Ma,  $57 \pm 7$  km of dextral slip accumulated across the Furnace Creek (38–48 km) and Stateline fault zones (13–16 km). Thus, we infer that whole-lithosphere shear initiated ca. 8–7 Ma. Greater net dextral shear ( $\sim 90$  km; 13–0 Ma) on the Furnace Creek ( $\sim 60$  km; Wernicke et al., 1988; Lutz, 2021) and Stateline fault zones ( $\sim 30$  km; Guest et al., 2007) suggests, in turn, that dextral shear before 8–7 Ma was confined to the upper crust. Early dextral slip was synchronous with early metamorphic core complex (MCC) exhumation, when the lithosphere was likely mechanically decoupled vertically (Fig. 4A).

Four independently derived Moho images (Fig. 1B; Figs. S5–S8) show generally northwest-increasing Moho depth, with apparent dextral offsets below the Furnace Creek and Stateline fault zones and above a deflection of the LAB depth gradient (described next). Southeast-decreasing Moho depth probably reflects southeast-increasing depth of exposure in the Mojave block, relative to the DVR, due to Laramide surficial erosion above the track of

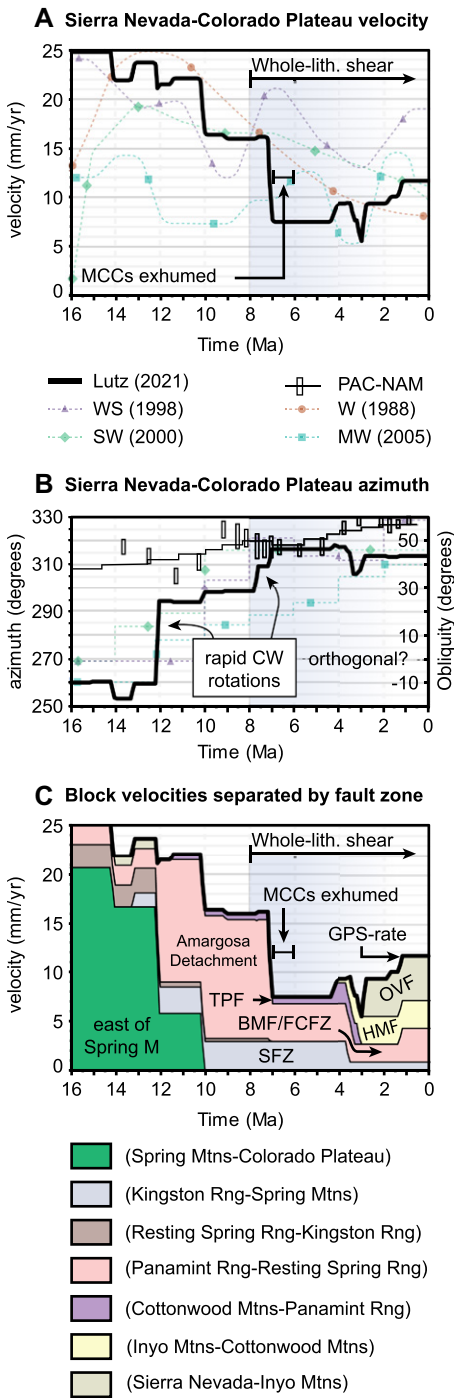


**Figure 2.** (A,C) Magnitude, and (B) azimuth, of relative velocity between the Sierra Nevada and Colorado Plateau from kinematic reconstructions. WS (1998)—Wernicke and Snow (1998); SW (2000)—Snow and Wernicke (2000); W (1988)—Wernicke et al. (1988); MW (2005)—McQuarrie and Wernicke (2005). Obliquity estimate (B) assumes north-south rift axis, consistent with the greater Basin and Range. Bold top line in C is net magnitude. Colors in C show specific fault-bounded block separations, with blocks labeled in explanation and separating fault abbreviated on plot. See Figures S1 and S2 (see footnote 1) for block locations. PAC-NAM—Pacific-North America azimuth (DeMets and Merkuriev, 2016); TPF—Towne Pass fault; MCCs—metamorphic core complexes; CW—clockwise; GPS—global positioning system; Rng—Range; Mtns—Mountains. See text and Figure 1 caption for other abbreviations.

gradient separates thicker (60–80 km) lithosphere to the northwest from thinner ( $\leq 60$  km) lithosphere to the southeast (Levander and Miller, 2012). We propose that the depth gradient was initially quasilinear, trended east-northeast, and formed during Late Cretaceous flat-slab erosion of the basal mantle lithosphere to the southeast (Saleeby, 2003; Axen et al., 2018). The initial east-northeast trend ( $\sim 071^\circ$  azimuth; Fig. 1C) is consistent with basal erosion during flat-slab subduction along the northwest edge of the initially east-northeast-moving ( $\sim 066^\circ$  azimuth) conjugate Shatsky Rise (Fig. 1C; Liu et al., 2010). If so, the originally northeast-trending LAB depth gradient defines the northwest extent of flat-slab erosion above the oceanic plateau.

We thus infer that the central, northwest-trending part of the LAB depth gradient was produced by dextral deflection of the older northeast-trending gradient. The gradient is steeper beneath Death Valley than northeast of the whole-lithosphere shear zone (Fig. 1C), which may be explained by dextral juxtaposition of thinner lithosphere to the southwest against thicker lithosphere to the northeast. Simple cut-and-slide reconstruction of the east-northeast-trending LAB depth gradient yielded  $56 \pm 6$  km of lower-lithosphere dextral shear (Fig. S4).

### Midcrustal Strengthening and Mechanical Coupling

Midcrustal strengthening is recorded by exhumation and cooling of MCCs in the DVR, which were mostly complete by ca. 8–6 Ma. At this time, midcrustal rocks in the Funeral and Black Mountains MCCs (blue in Figs. 1A and 3; also see Fig. S1 for range names) cooled through  $\sim 200^\circ\text{C}$  during rapid detachment-related exhumation (Fig. S3C). Thermo-kinematic (two-dimensional) (Lutz et al., 2021) and thermal (one-dimensional) (e.g., Bidgoli et al., 2015) modeling of this exhumation showed major (40–70  $^\circ\text{C}/\text{m.y.}$ ) MCC cooling from ca. 10 to 6 Ma. Exhumation-related midcrustal cooling and thinning strengthened the middle crust

the conjugate Shatsky Rise (see flat-slab azimuth in Fig. 1C), as recorded by thermochronology (see Saleeby, 2003). Each Moho image shows a dextral-sense deflection or offset beneath the Furnace Creek and Stateline fault zones. Reconstructions of the four Moho depth gradients yielded various magnitudes (Table S5) that, combined, suggest  $62 \pm 17.5$  km of lower-crustal dextral shear.

A generally northeast-trending LAB depth gradient, with a central northwest-trending section below the DVR (Figs. 1C and 4), is imaged robustly (Levander and Miller, 2012). The LAB

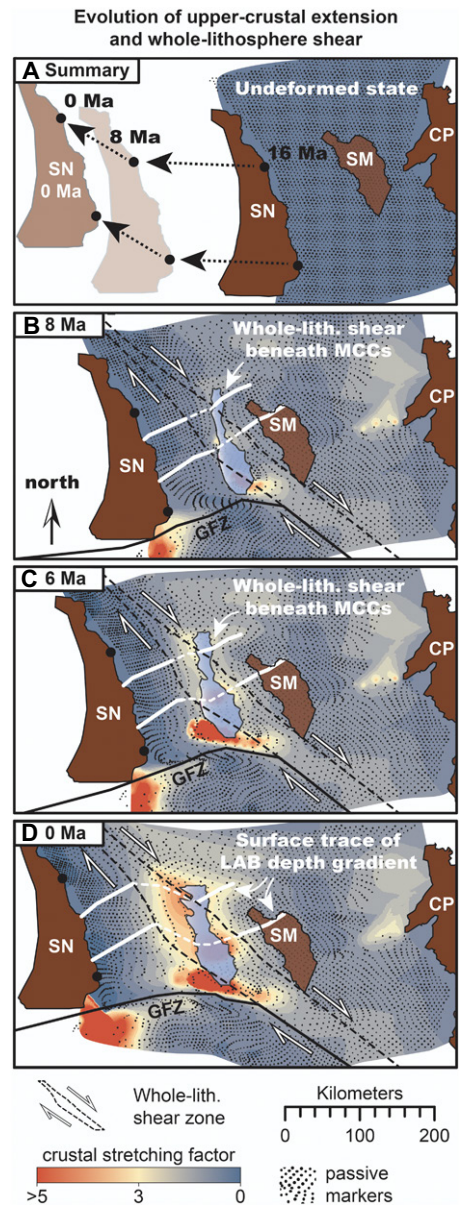


**Figure 3.** Snapshots of the kinematic model of Lutz (2021) showing evolution of upper-crustal stretching factor and whole-lithosphere shear. Black dots are passive markers that translate with modeled fault blocks (not shown; see Video S1 [see footnote 1]). Triangulated mesh between passive markers was used to calculate net accrued crustal stretching factors (e.g., Müller et al., 2018). Dashed arrows in A are incremental motion vectors of the Sierra Nevada (SN) relative to the Colorado Plateau (CP). Note that lithosphere-asthenosphere boundary (LAB) depth gradient (thick white and dashed lines in B–D) is deflected only in the zone of maximum upper-crustal stretching near the metamorphic core complexes (MCCs). GFZ—Garlock fault zone; SM—Spring Mountains.

beneath DVR MCCs, leading to whole-lithosphere mechanical coupling (Lutz et al., 2021).

Existing studies with diverse approaches support the presence of a mechanically coupled lithosphere in the DVR. Park and Wernicke

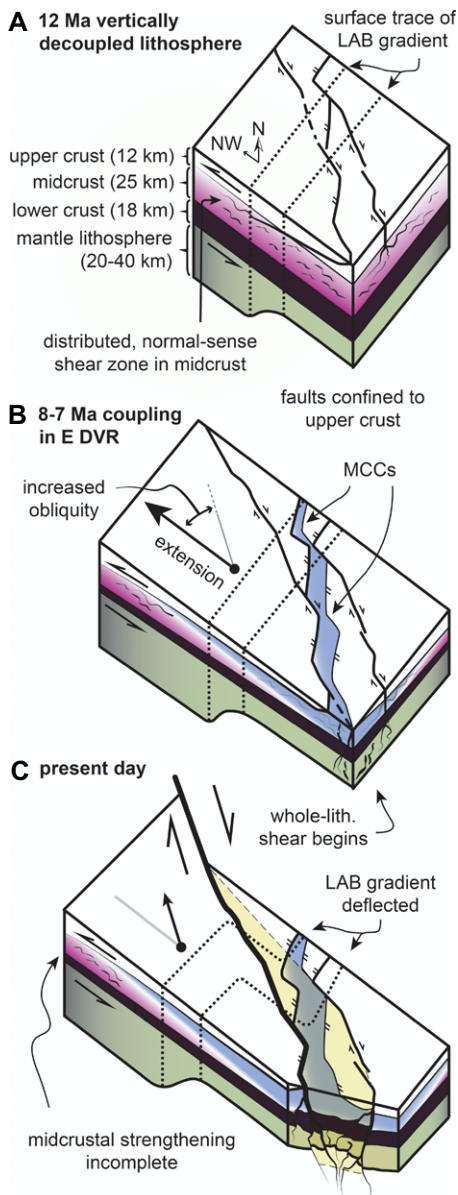


**Figure 4.** Conceptual model for whole-lithosphere shear during oblique rifting in the Death Valley region (DVR). (A) 12 Ma decoupled extension. LAB—lithosphere-asthenosphere boundary. (B) Ca. 8–7 Ma midcrustal (MC) strengthening coupled upper crust (UC) to lower crust/mantle lithosphere (LCML), enabling whole-lithosphere shear. MCCs—metamorphic core complexes. (C) Present day, showing whole-lithosphere shear zone (light yellow in map view). Pink middle crust indicates weak, decoupling behavior, whereas blue indicates strengthened middle crust.

(2003) concluded from magnetotelluric surveying that the whole lithosphere is well coupled in the eastern DVR and that a conductive zone extending to 20 km depth beneath Death Valley is due to dextral transtensive faulting. Uppermost mantle xenoliths in our inferred zone of whole-lithosphere shear (Cima volcanic field; Fig. 1A) are interpreted to have been sheared in Pliocene time (Behr and Hirth, 2014). Modeling

suggests that LCML visco-plastic shear under the DVR is subparallel to our whole-lithosphere shear zone (Barbot, 2020).

### CONTROLS ON WHOLE-LITHOSPHERE SHEAR

We conclude that (1) initiation of whole-lithosphere dextral shear in the eastern DVR was controlled spatiotemporally by midcrustal strengthening, (2) this dextral shear was likely assisted by increased obliquity, and (3) increased regional strain rate was not a factor. The DVR extension direction (and obliquity, if the rift axis is considered to trend approximately north-south) rotated  $\sim 18^\circ$  clockwise into parallelism with Pacific–North American relative plate motion at ca. 8–7 Ma (Figs. 2B, 3A, 4B, and 4C), coeval with the proposed onset of whole-lithosphere shear. However, increased obliquity at ca. 7 Ma did not produce whole-lithosphere shear zones across the region. Instead, whole-lithosphere shear localized beneath detachment-dominated areas in the eastern DVR (Figs. 1A and 3B–3D), where the lithosphere was preconditioned for integrated failure by midcrustal strengthening. Thus, we argue that increased rift obliquity was of secondary importance, and we argue that a weak midcrust persists west of the MCC belt, where crust is relatively thick (Fig. 1B) and the LAB depth gradient still trends northeast (Fig. 1C). If correct, then upper-crustal strike-slip motion west of the MCCs remains decoupled from shear in the LCML (Fig. 4C). The apparent lack of whole-lithosphere shear in the western DVR supports the importance of midcrustal strengthening as a control on whole-lithosphere shear: high strain rate (Fig. 2C), high obliquity (Fig. 2B), and the presence of a major preexisting crustal shear zone (Kylander-Clark et al., 2005) apparently have not overcome the decoupling effect of weak middle crust.

It is possible that the whole-lithosphere shear zone defined here reactivated a hypothetical preexisting, northwest-southeast-trending weak zone in the LCML that became well oriented for slip after ca. 8–7 Ma. However, such a weak zone did not exist in the upper crust, where many north- to northeast-trending Permian–Jurassic thrusts were continuous across the shear zone before that time (e.g., Wernicke et al., 1988; Lutz et al., 2021).

Midcrustal strengthening and mechanical coupling of the upper crust and LCML may have favored progressive dextral strain in the LCML via associated weakening feedbacks. For example, seismic slip or rapid creep events propagating downward into, and episodically loading, the LCML would likely weaken it by cataclastic grain-size reduction, hydrous alteration, and shear heating. These processes, in turn, would accelerate diffusion and dissolution creep and the development and/or dispersal of weak phyllosilicates, weakening ductile shear zones and favoring strain

localization in the LCML (e.g., Platt and Behr, 2011; Montési, 2013). Strong coupling between the upper crust and LCML may be required to establish this strain-weakening feedback loop between slow loading by mantle flow and episodic seismic loading by brittle faulting (Cowie et al., 2013; Chatzaras et al., 2015). Such coupling relies in turn upon midcrustal strengthening if crust was previously thick.

### ACKNOWLEDGMENTS

The authors were supported by National Science Foundation grant EAR-1516680. Reviews by Brian Wernicke, Sascha Brune, and an anonymous reviewer are greatly appreciated. Discussions with Terry Pavlis, Michael Wells, and Basil Tikoff improved the manuscript. This work would not have been possible without EarthScope (<https://www.earthscope.org>) and EarthByte (<https://www.earthbyte.org>). This is Los Alamos National Laboratory contribution LA-UR-21-28189.

### REFERENCES CITED

- Axen, G.J., van Wijk, J.W., and Currie, C.A., 2018, Basal continental mantle lithosphere displaced by flat-slab subduction: *Nature Geoscience*, v. 11, p. 961–964, <https://doi.org/10.1038/s41561-018-0263-9>.
- Barbot, S., 2020, Mantle flow distribution beneath the California margin: *Nature Communications*, v. 11, p. 4456, <https://doi.org/10.1038/s41467-020-18260-8>.
- Behr, W.M., and Hirth, G., 2014, Rheological properties of the mantle lid beneath the Mojave region in southern California: *Earth and Planetary Science Letters*, v. 393, p. 60–72, <https://doi.org/10.1016/j.epsl.2014.02.039>.
- Bennett, S.E.K., and Oskoin, M.E., 2014, Oblique rifting ruptures continents: Example from the Gulf of California shear zone: *Geology*, v. 42, p. 215–218, <https://doi.org/10.1130/G34904.1>.
- Bigdoli, T.S., Amir, E., Walker, J.D., Stockli, D.F., Andrew, J.E., and Caskey, S.J., 2015, Low-temperature thermochronology of the Black and Panamint Mountains, Death Valley, California: Implications for geodynamic controls on Cenozoic intraplate strain: *Lithosphere*, v. 7, p. 473–480, <https://doi.org/10.1130/L406.1>.
- Block, L., and Royden, L.H., 1990, Core complex geometries and regional scale flow in the lower crust: *Tectonics*, v. 9, p. 557–567, <https://doi.org/10.1029/TC009i004p0557>.
- Brune, S., Popov, A.A., and Sobolev, S.V., 2012, Modeling suggests that oblique extension facilitates rifting and continental break-up: *Journal of Geophysical Research: Solid Earth*, v. 117, B08402, <https://doi.org/10.1029/2011JB008860>.
- Buck, W.R., 1991, Modes of continental lithospheric extension: *Journal of Geophysical Research: Solid Earth*, v. 96, B12, p. 20,161–20,178, <https://doi.org/10.1029/91JB01485>.
- Burchfiel, B.C., and Royden, L.H., 1985, North-south extension within the convergent Himalayan region: *Geology*, v. 13, p. 679–682, [https://doi.org/10.1130/0091-7613\(1985\)13<679:NEW TCH>2.0.CO;2](https://doi.org/10.1130/0091-7613(1985)13<679:NEW TCH>2.0.CO;2).
- Chatzaras, V., Tikoff, B., Newman, J., Withers, A.C., and Drury, M.R., 2015, Mantle strength of the San Andreas fault system and the role of mantle-crust feedbacks: *Geology*, v. 43, p. 891–894, <https://doi.org/10.1130/G36752.1>.
- Cowie, P.A., Scholz, C.H., Roberts, G.P., Walker, J.F., and Steer, P., 2013, Viscous roots of active seismic faults revealed by geologic slip rate vari-

- ations: *Nature Geoscience*, v. 6, p. 1036–1040, <https://doi.org/10.1038/ngeo1991>.
- DeMets, C., and Merkouriev, S., 2016, High-resolution reconstructions of Pacific–North America plate motion: 20 Ma to present: *Geophysical Journal International*, v. 207, p. 741–773, <https://doi.org/10.1093/gji/ggw305>.
- Dixon, T.H., and Xie, S., 2018, A kinematic model for the evolution of the Eastern California shear zone and Garlock fault, Mojave Desert, California: *Earth and Planetary Science Letters*, v. 494, p. 60–68, <https://doi.org/10.1016/j.epsl.2018.04.050>.
- Gilbert, H., 2012, Crustal structure and signatures of recent tectonism as influenced by ancient terranes in the western United States: *Geosphere*, v. 8, p. 141–157, <https://doi.org/10.1130/GES00720.1>.
- Guest, B., Niemi, N., and Wernicke, B.P., 2007, Stateline fault system: A new component of the Miocene–Quaternary Eastern California shear zone: *Geological Society of America Bulletin*, v. 119, p. 1337–1347, [https://doi.org/10.1130/0016-7606\(2007\)119\[1337:SFSA NC\]2.0.CO;2](https://doi.org/10.1130/0016-7606(2007)119[1337:SFSA NC]2.0.CO;2).
- Kylander-Clark, A.R.C., Coleman, D.S., Glazner, A.F., and Bartley, J.M., 2005, Evidence for 65 km of dextral slip across Owens Valley, California, since 83 Ma: *Geological Society of America Bulletin*, v. 117, p. 962–968, <https://doi.org/10.1130/B25624.1>.
- Levander, A., and Miller, M.S., 2012, Evolutionary aspects of lithosphere discontinuity structure in the western U.S.: *Geochemistry Geophysics Geosystems*, v. 13, Q0AK07, <https://doi.org/10.1029/2012GC004056>.
- Liu, L., Gurnis, M., Seton, M., Saleeby, J., Müller, R.D., and Jackson, J.M., 2010, The role of oceanic plateau subduction in the Laramide orogeny: *Nature Geoscience*, v. 3, p. 353–357, <https://doi.org/10.1038/ngeo829>.
- Lutz, B.M., 2021, Large-Magnitude Extension in the Death Valley Region, SW USA: Thermo-Kinematic Modeling, Whole-Lithosphere Shear, and Disruption of Drainage Systems [Ph.D. thesis]: Socorro, New Mexico, New Mexico Institute of Mining and Technology, 198 p.
- Lutz, B.M., Ketcham, R.A., Axen, G.J., Beyene, M.A., Wells, M.L., van Wijk, J.W., Stockli, D.F., and Ross, J.I., 2021, Thermo-kinematic modeling of detachment-dominated extension, northeastern Death Valley area, USA: Implications for mid-crustal thermal-rheological evolution: *Tectonophysics*, v. 808, 228755, <https://doi.org/10.1016/j.tecto.2021.228755>.
- McQuarrie, N., and Wernicke, B.P., 2005, An animated tectonic reconstruction of southwestern North America since 36 Ma: *Geosphere*, v. 1, p. 147–172, <https://doi.org/10.1130/GES00016.1>.
- Montési, L.G.J., 2013, Fabric development as the key for forming ductile shear zones and enabling plate tectonics: *Journal of Structural Geology*, v. 50, p. 254–266, <https://doi.org/10.1016/j.jsg.2012.12.011>.
- Müller, R.D., Cannon, J., Qin, X., Watson, R.J., Gurnis, M., Williams, S., Pfaffelmoser, T., Seton, M., Russell, S.H.J., and Zahirovic, S., 2018, GPlates: Building a virtual Earth through deep time: *Geochemistry Geophysics Geosystems*, v. 19, p. 2243–2261, <https://doi.org/10.1029/2018GC007584>.
- Oakes, E.H., 1987, Age and rates of displacement along the Furnace Creek fault zone, northern Death Valley, California: *Geological Society of America Abstracts with Programs*, v. 14, no. 437, p. 378.
- Oskin, M., and Stock, J., 2003, Pacific–North America plate motion and opening of the Upper Delfin basin, northern Gulf of California, Mexico: *Geological Society of America Bulletin*, v. 115, p. 1173–1190, <https://doi.org/10.1130/B25154.1>.
- Oskin, M., Stock, J., and Martín-Barajas, A., 2001, Rapid localization of Pacific–North America plate motion in the Gulf of California: *Geology*, v. 29, p. 459–462, [https://doi.org/10.1130/0091-7613\(2001\)029<0459:RLO PNA>2.0.CO;2](https://doi.org/10.1130/0091-7613(2001)029<0459:RLO PNA>2.0.CO;2).
- Park, S.K., and Wernicke, B.P., 2003, Electrical conductivity images of Quaternary faults and Tertiary detachments in the California Basin and Range: *Tectonics*, v. 22, 1030, <https://doi.org/10.1029/2001tc001324>.
- Pérez-Gussinyé, M., and Reston, T.J., 2001, Rheological evolution during extension at nonvolcanic rifted margins: Onset of serpentinization and development of detachments leading to continental breakup: *Journal of Geophysical Research: Solid Earth*, v. 106, B3, p. 3961–3975, <https://doi.org/10.1029/2000JB900325>.
- Platt, J.P., and Behr, W.M., 2011, Grain-size evolution in ductile shear zones: Implications for strain localization and the strength of the lithosphere: *Journal of Structural Geology*, v. 33, p. 537–550, <https://doi.org/10.1016/j.jsg.2011.01.018>.
- Rosenbaum, G., Regenauer-Lieb, K., and Weinberg, R., 2005, Continental extension: From core complexes to rigid block faulting: *Geology*, v. 33, p. 609–612, <https://doi.org/10.1130/G21477.1>.
- Saleeby, J., 2003, Segmentation of the Laramide slab—Evidence from the southern Sierra Nevada region: *Geological Society of America Bulletin*, v. 115, p. 655–668, [https://doi.org/10.1130/0016-7606\(2003\)115<0655:SOTLSF>2.0.CO;2](https://doi.org/10.1130/0016-7606(2003)115<0655:SOTLSF>2.0.CO;2).
- Snow, J.K., and Wernicke, B.P., 2000, Cenozoic tectonism in the central Basin and Range: Magnitude, rate, and distribution of upper crustal strain: *American Journal of Science*, v. 300, p. 659–719, <https://doi.org/10.2475/ajs.300.9.659>.
- Sobolev, S.V., Petrunin, A.G., Garfunkel, Z., and Babeyko, A., 2005, Thermo-mechanical model of the Dead Sea Transform: *Earth and Planetary Science Letters*, v. 238, p. 78–95, <https://doi.org/10.1016/j.epsl.2005.06.058>.
- Umhoefer, P.J., 2011, Why did the southern Gulf of California rupture so rapidly?—Oblique divergence across hot, weak lithosphere along a tectonically active margin: *GSA Today*, v. 21, no. 11, p. 4–10, <https://doi.org/10.1130/G133A.1>.
- Wernicke, B., 1992, Cenozoic extensional tectonics of the U.S. Cordillera, in Burchfiel, B.C., et al., eds., *The Cordilleran Orogen: Conterminous U.S.: Boulder, Colorado, Geological Society of America, The Geology of North America*, v. G-3, p. 553–581, <https://doi.org/10.1130/DNAG-GNA-G3.553>.
- Wernicke, B.P., and Snow, J.K., 1998, Cenozoic tectonism in the central Basin and Range: Motion of the Sierran–Great Valley block: *International Geology Review*, v. 40, p. 403–410, <https://doi.org/10.1080/00206819809465217>.
- Wernicke, B.P., Axen, G.J., and Snow, J.K., 1988, Basin and Range extensional tectonics at the latitude of Las Vegas, Nevada: *Geological Society of America Bulletin*, v. 100, p. 1738–1757, [https://doi.org/10.1130/0016-7606\(1988\)100<1738:BA RETA>2.3.CO;2](https://doi.org/10.1130/0016-7606(1988)100<1738:BA RETA>2.3.CO;2).

Printed in USA